STUDIA UBB CHEMIA, LXI, 1, 2016 (p. 163-175)
(RECOMMENDED CITATION)

Dedicated to Professor Mircea Diudea on the Occasion of His 65th Anniversary

OPTIMAL CONDITIONS FOR PREPARING CIGS THIN FILM THROUGH TWO-STEPPROCESS OF SPUTTERING FOLLOWED BY SELENIZATION

M. MORADI[a], M. ZAHEDIFAR[a,b], T. GHORBANI[a,*], M. SAADAT[a], K. ROSTAMI[a]

ABSTRACT. Cu(In,Ga)Se_2 films were prepared via a sputtering route followed by a selenization process, on glass substrates. Having a layer sequence Mo/In/Cu-Ga with preferred thicknesses, the metallic layers were selenized at vacuum of 6×10^{-3} mbar and 1 atm pressure with a total gas inlet of 7 sccm. Under vacuum, only single-phase CIGS was observed while at 1 atm, other phases in addition to CIGS were formed. The metallic layers were selenized at several temperatures. Pure-phased CIGS films were obtained by selenization at 600˚C. The crystallinity of the obtained films was further enhanced by increasing the selenization temperature. The produced CIGS films were studied by X-ray diffraction (*XRD*), scanning electron microscope (*SEM*) and energy dispersion spectroscopy (*EDS*) techniques.

Keywords: *Cu(In,Ga)Se_2 thin film, sputtering, selenization.*

INTRODUCTION

Chalcopyrite $CuInGaSe_2$ (CIGS), due to its high absorption coefficient ($\alpha\sim10^5$ cm^{-1}), is one of the most promising absorber materials for thin film solar cells tunable band gap and long-term stability [1, 2]. The band gap of $CuInSe_2$ is E_g=1 eV and that of $CuGaSe_2$ is1.7 eV. Therefore, a manipulation of the band gap between these two extremes makes it possible to prepare a wide variety

[a] *Institute of Nanoscience and Nanotechnology, University of Kashan, Kashan, Iran*
[b] *Physics Department, University of Kashan, Kashan, Iran*
* *Corresponding Author: ghorbani.tayebeh@gmail.com*

of absorber materials by simply adjusting the Ga/In ratio [3]. Here, the gallium ratio (Ga/(Ga + In)) could be adjusted by changing the thicknesses of the In and Cu-Ga films. The optimal Cu/(In+Ga) elemental ratio is typically between 0.8 to 0.9 [4,5] and that of Ga/In is about 0.3 corresponding to a band gap of 1.1 eV [6]. The hypothetical efficiency of polycrystalline solar cells increase with increasing the grain size of the absorber materials. Various methods such as chemical bath deposition [7], elemental co-evaporation [8], flash evaporation [9], single-source evaporation [10], RF sputtering [11,12], pulsed laser deposition [13], andelectrodeposition [14,15] have been used to prepare CIGS thin films.

Another method to fabricate CIGS films is a two-step process, wherein the metallic films are deposited as the precursor films via the sputtering method followed by the selenization process. The first advantage of this method is that no precise control of the parameters is needed during the selenization process, as the metallic precursors absorb only the amount of selenium required by the stoichiometry [16-18]. The second is diffusion of Se into the Mo back-contact, thereby $MoSe_2$ is formed at the boundary of the active layer and the back-contact leading to an improved junction between the two materials [19]. The surface roughness of the absorber plays a vital role to form p–n junction between the absorber and window layer. A thin absorber layer with rough surface produces shunt path in the devices. On the other hand, a very smooth surface is not applicable because of reflection losses [4]. In this work, CIGS thin films were synthesized using the sputtering and post-selenization method. The layer sequence Mo/In/Cu-Ga with two different thicknesses was tested. The influence of annealing temperature and pressure were investigated and their optimum conditions for producing CIGS thin films were explored. The surface roughness of the prepared samples was also studied and the optimal conditions were obtained for the fabricated CIGS layer.

EXPERIMENTAL

Soda lime glass (SLG) substrates of 11 × 26 mm^2 area and 1 mm thick were used for deposition. The substrates were scoured using detergent and ultrasonic cleaning by deionized water and acetone, followed by scrubbing with iso-propanol, drying with N_2 gas and immediately introducing into the vacuum chamber. Molybdenum (Mo) layer was deposited as back contact by RF magnetron sputtering onto the SLG substrate. Copper/Gallium (75:25 at%) alloy and pure indium targets were sequentially used for depositing the precursor films on SLG substrates via the sputtering route employing a RF magnetron sputtering system. The distance between the target and substrate was 20 cm and the substrates were fixed during deposition. The target power and voltage

were 250 W and 290 V respectively. In order to develop the CIGS films, the multi-layered precursor stacks were selenized in a closed steel container, where the evaporated selenium was loaded into an argon flux in a quartz tube. Selenium was supplied by placing 1.0 g of elemental selenium into the box prior to heating. The layer sequence Mo/In/Cu-Ga with two different thicknesses were tested: 300 nm/300 nm/160 nm (sample A) and 300 nm/300 nm/275 nm (sample B). Selenization procedure was carried out according to time-temperature profile shown in Figure 1.

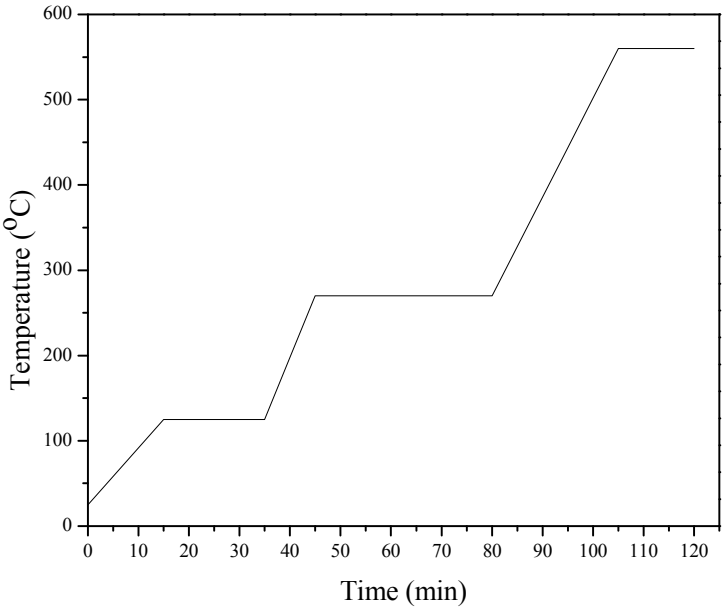

Figure 1. Schematic temperature profile used in selenization process.

The first step at 125 ˚C was conducted to obtain a good Cu–In/Ga alloy with stable physical properties [20]. In the second step, Se incorporation was allowed to diffuse into the alloy layer at 250 ˚C. The third step, was involved selenization and recrystallization process which was performed at an elevated temperature of 550 ˚C [21]. In order to investigate the atmosphere effect, the selenization process of sample B was performed at two conditions. First one at pressure of 1 atm and the second at the vacuum of 6×10^{-3} mbar, with a total gas inlet of 7 sccm each. Figure1 demonstrates the Selenization process.

Annealing temperature effect was examined by conducting the selenization process in a gas inlet of 7 sccm and vacuum of 2×10^{-3} mbar at 400, 450, 500, 600, 700, 800 ˚C. Phase evolution of the precursor and selenized

specimens was analyzed using a X-ray powder diffractometer (XRD, Philips X'Pert/PMD) and Cu K_α radiation at 40 kV and 30 mA. The roughness of surface of the samples was studied by a Confocal Microscope. The scanning electron microscopy (SEM) and energy dispersive spectroscopy (EDS) measurements were carried out by a VEGA\\TESCAN microscope.

RESULTS AND DISCUSSION

Figure 2 shows a typical XRD pattern of absorber layer prepared by sequential sputtering of sample A. According to this figure, the formation of a monophase $CuInSe_2$ layer instead of CIGS phase, can be ascribed to low thickness of Cu-Ga layer. Therefore, the Cu-Ga layer thickness was increased to 275 nm (sample B).

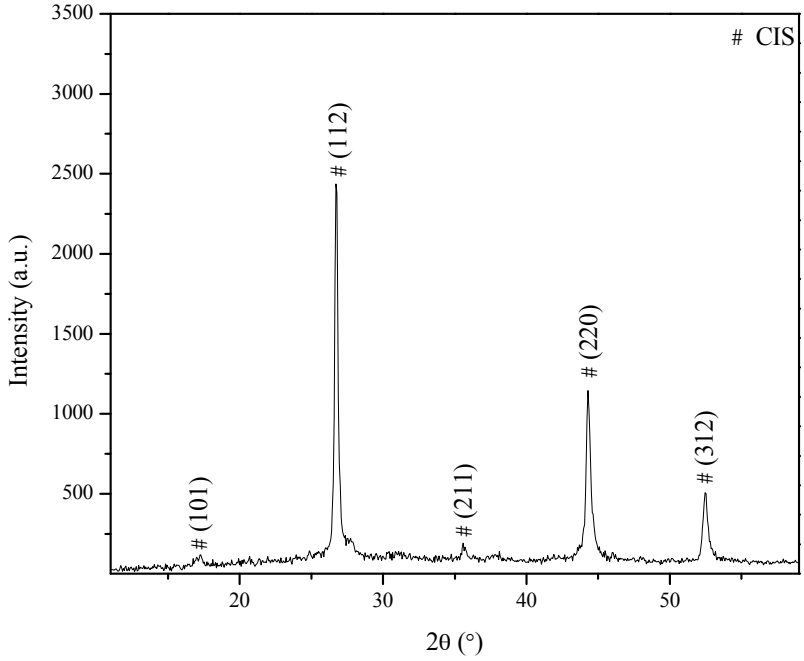

Figure 2. XRD patterns of sample A fairly coincides with that of single phase CIS thin film.

Figure 3 shows a typical XRD pattern of sample B, which reveals the main chalcopyrite diffraction peaks. The CIGS crystals with different compositions of Ga element have different positions of XRD reflection peaks.

The XRD pattern with two reflection peaks, indicates a non-uniform distribution Ga element in the $CuInGaSe_2$ absorber layer. The inset of Figure 3 shows an expanded view of positions of the (112) reflection peaks. The elemental composition distributions onto the surface and into the depth of the surface were investigated by EDS via two methods: Variation of EDS accelerating voltage and the cross-sectional depth composition of CIGS absorber. Variation of CIGS composition with EDS accelerating voltage is presented in Table 1. It is worth noting that gallium content increases from 0.29 near the surface to 1.92 at 25 kV which suggests diffusion of gallium toward the bottom of CIGS film.

Table **1**. Atomic percentage of sample B for different EDS accelerating voltages.

Accelerating voltage (kV)	Cu (at %)	Ga (at %)	Se (at %)	In (at %)
5	19.37	0.29	41.25	39.09
10	23.56	0.87	49.68	25.89
15	24.43	0.42	51.27	23.88
20	22.69	1.28	52.11	23.92
25	22.41	1.92	50.8	24.87

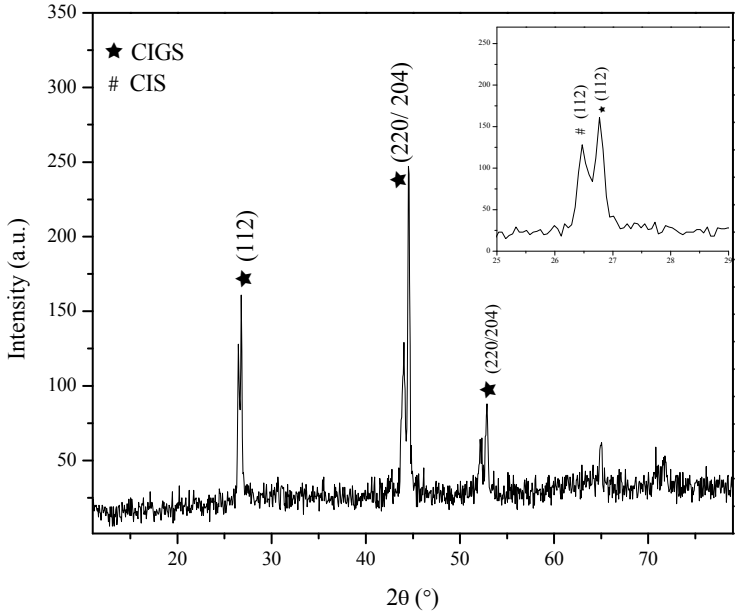

Figure 3. XRD patterns of CIGS thin film by sequential sputtering of sample B. The inset shows an expanded view of positions of the (112) reflection peak.

Figure 4 showing the cross-sectional depth composition of sample B is a result of EDS point analysis. The atomic concentrations measured by EDS analysis at 9 points are summarized in Table 2.

Table 2. The cross-sectional atomic % measured by EDS analysis at 9 points of sample B.

Point	Cu (%)	Ga (%)	Se (%)	In (%)
1	21.49	22.2	41.43	14.88
2	23.29	10.33	47.78	18.6
3	21.93	12.4	48.13	17.54
4	18.42	5.47	53.6	22.51
5	16.99	3.5	57.07	22.44
6	19.52	4.19	55.28	21.01
7	14.28	5.68	55.91	24.13
8	18.58	4.75	55.06	21.61
9	17.72	4.22	57.62	20.44

It is observed that the atomic concentration is considerably different along the depth, such that the Ga (In) concentration increases (decreases) slowly from the surface to the dept. Also apparent in Table 2 is that the amount of Se on the surface of CIGS film is larger than that in the interior, where the Cu concentration increases slowly from the surface to the inside.

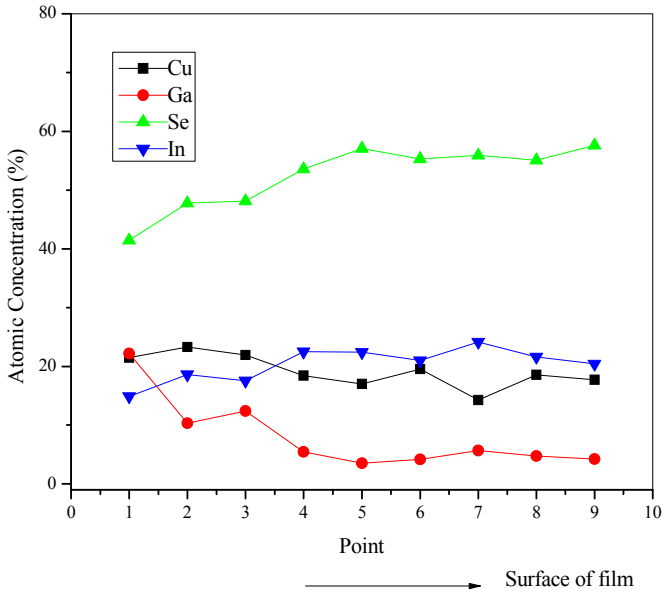

Figure 4. The EDS depth composition point analysis of sample B.

Figure 5 shows the SEM cross-section and top view of sample B. The film is dense and polycrystalline with compact 'facet-shaped' texture grain.

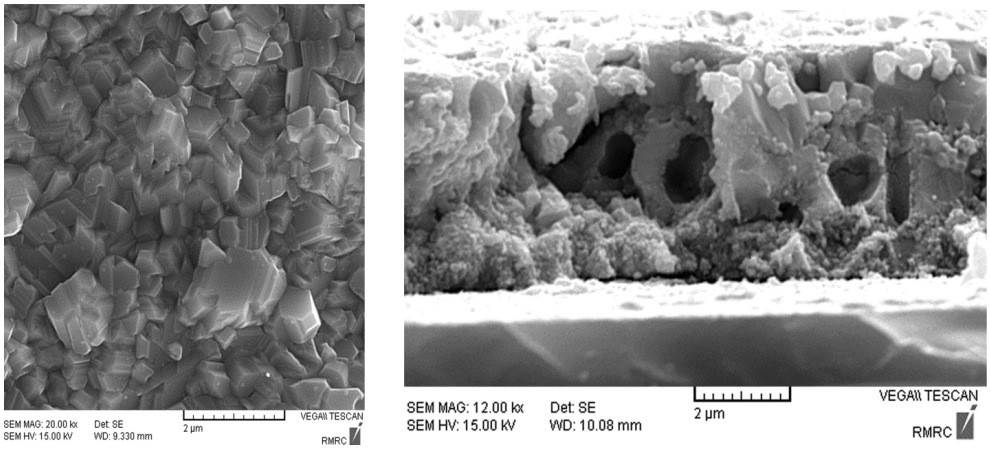

Figure 5. SEM cross-section and top view of sample B.

Figures 6 and 7 illustrate the X-ray diffraction patterns of sample B selenized respectively at the pressure of 10^{-3} mbar (medium vacuum) and 1000 mbar (atmosphere), each for 0.5 h. Under vacuum, only single-phase CIGS was observed but at 1 atm, other phases such as In_2O_3 compound was formed in addition to CIGS, which is due to presence of oxygen in the environment. Table 3 shows the EDS analysis of the sample selenized at 1 atm for 0.5 h.

Figure 8 illustrates the X-ray diffraction patterns of sample B selenized at various temperatures for 0.5h. Despite of formation of CIGS film following selenization at 400 ˚C, In_2Se_3 and Cu_2In were also present in the sample. By increasing the selenization temperature to 450 ˚C, In_2CuO_4 and In_2O_3 were found to coexist with CIGS in the prepared film. At 500 ˚C, CuO and CIGS phases were formed. Monophasic CIGS was obtained by rising the selenization temperature to 600 ˚C. The crystallinity of the obtained film was further enhanced by increasing the selenization temperature to 700 ˚C.

Table 3. EDS analysis of sample B selenized at 1 atm for 0.5 h.

Element	O	Cu	Ga	Se	In
Atomic (%)	8.88	31.91	0.44	34.26	24.51

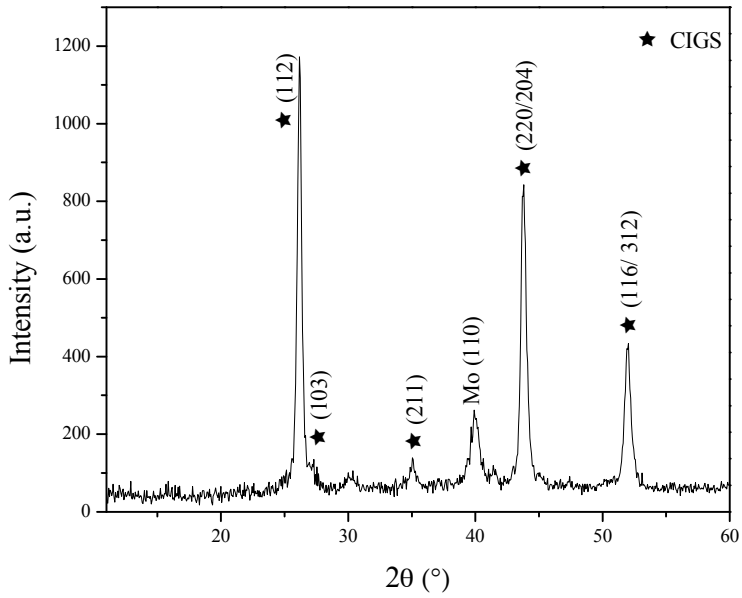

Figure 6. X-ray diffraction patterns of sample B selenized at pressure 10^{-3} mbar.

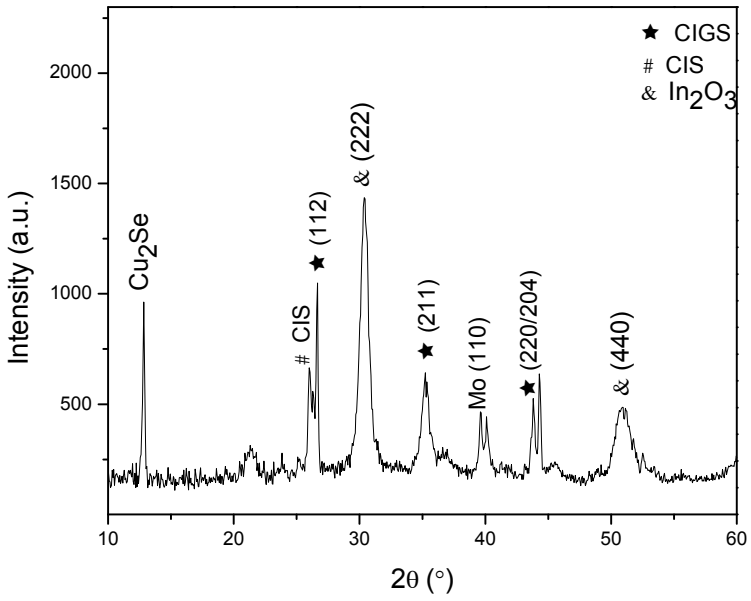

Figure 7. X-ray diffraction patterns of sample B selenized at 1 atm.

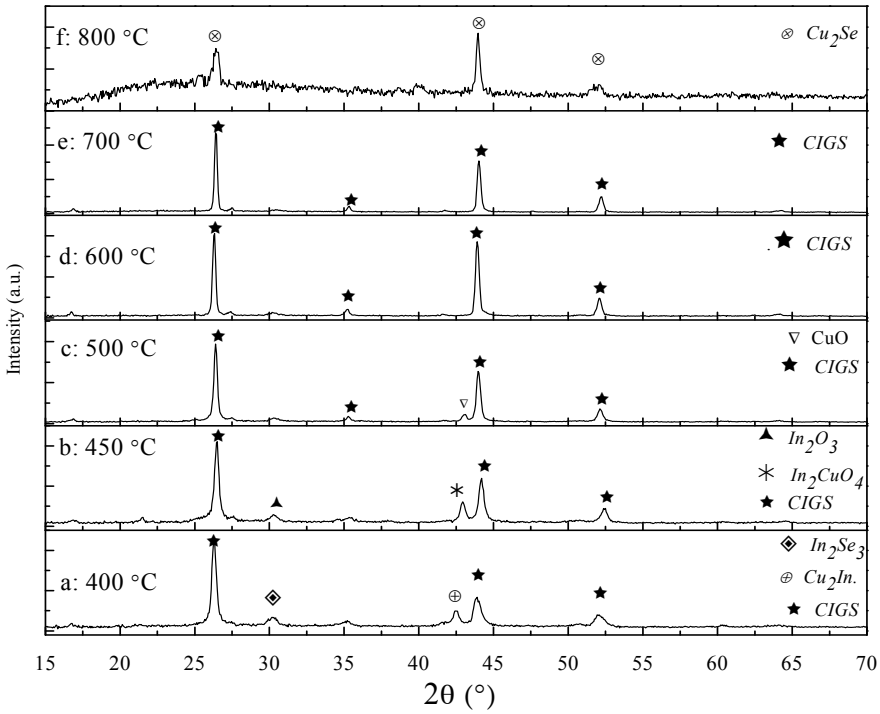

Figure 8. X-ray diffraction patterns of sample B selenized at different temperatures for 0.5h.

With more escalating the selenization temperature up to 800 ˚C, the CIGS phase disappeared, Cu_2Se was formed and the layer became amorphous like.

CIGS films were successfully formed at the selenization temperature of 450 ˚C. It was observed that increasing the selenization temperature from 400 to 450 ˚C resulted in a shift of the (112) diffraction peak toward higher angles. It was because Ga ions incorporated into CIGS to substitute indium ions, so that the lattice constants decreased due to the substitution of large In ion by small Ga ion [22]. Further increasing the temperatures led to increased intensity of (112) peak while its position shifted slightly to lower angles, justifying the sample selenized at 450 ˚C has the most Ga content.

Figure 9 shows the SEM cross-section and top view of sample B selenized at 400, 450, 500 and 700 ˚C. When the temperature of selenization increased, the geometry of the grain was changed from an agglomerated shape to a more compact ‘facet-shaped’ texture, and the crystallite size markedly increased. Selenization at 700 ˚C produced delamination of the CIGS absorber layer.

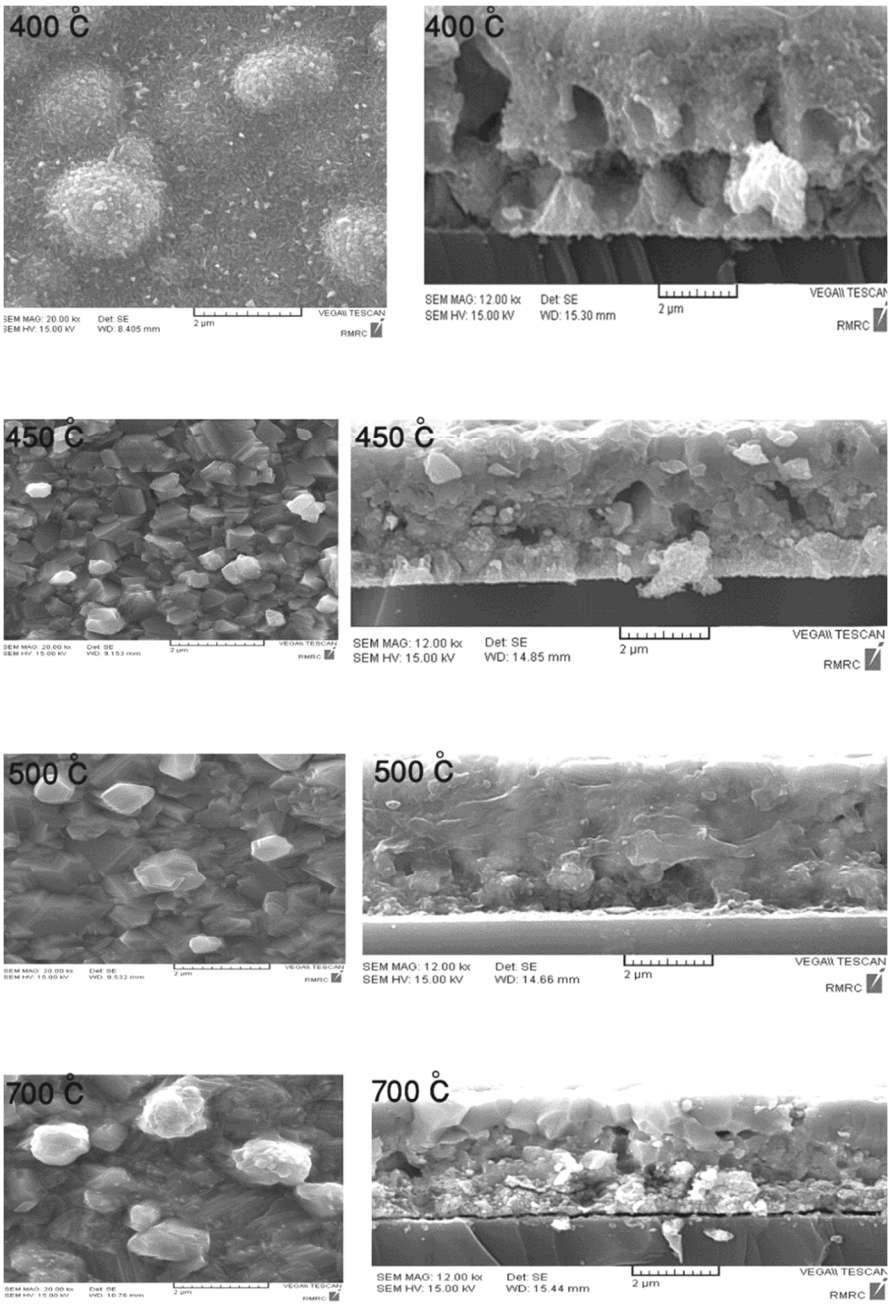

Figure 9. SEM cross-section (right) and top view (left) of sample B selenized at various temperatures for 0.5h.

Figure 10 shows the surface roughness of sample B selenized at 400, 450, 500, 700 and 800 ˚C. The sample selenized at 400 ˚C has the lowest surface roughness, which could be due to presence of other phases. The decrease in surface roughness of CIGS layers with increasing selenizing temperature from 500 to 700 ˚C can be attributed to growing the grain size in higher temperature. At 800 ˚C the layer destroyed completely.

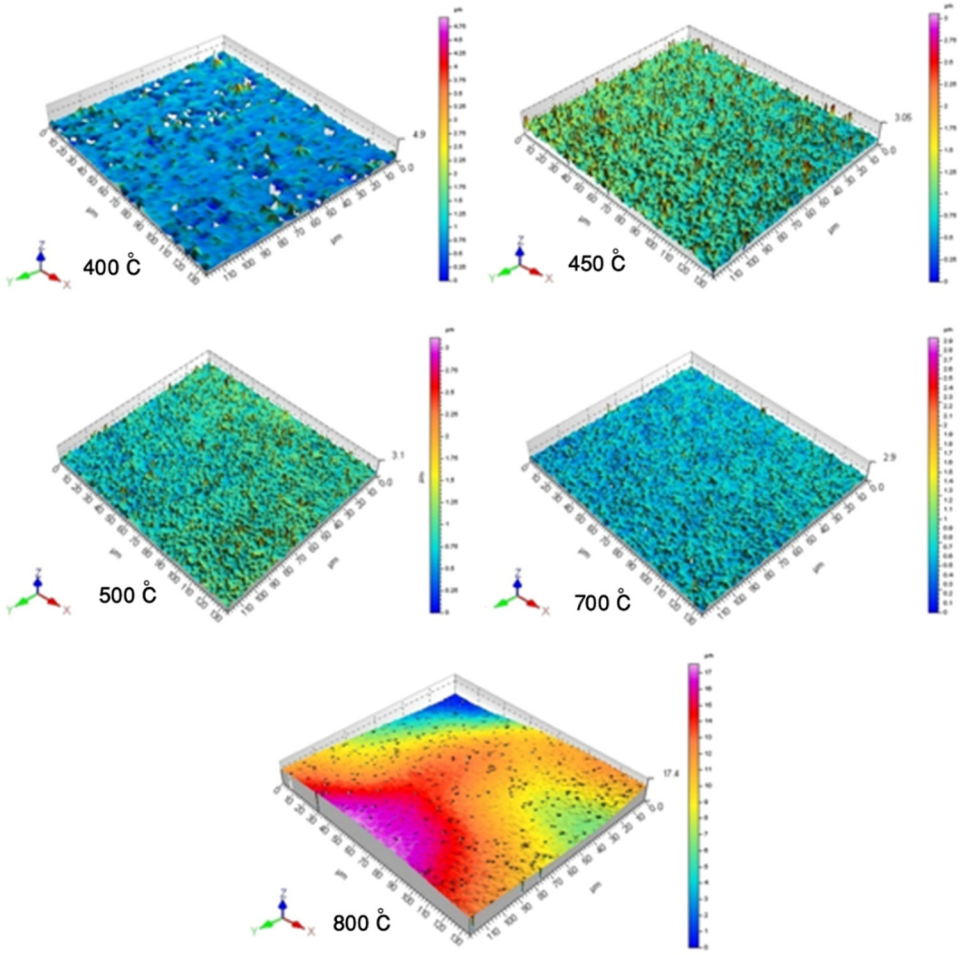

Figure 10. Surface roughness of sample B selenized at 400, 450, 500, 700 and 800 ˚C.

CONCLUSIONS

$Cu(In,Ga)Se_2$ films were prepared via the sputtering method followed by selenization process. Two samples with different Cu-Ga thicknesses of 160 and 275 nm were tested. In the former case, monophasic $CuInSe_2$ was obtained instead of CIGS phase and in the latter, CIGS was formed. By selenizing the samples prepared with 275 nm Cu-Ga at 1 atm, In_2O_3 compound in addition to CIGS were appeared but under vacuum, only single-phase CIGS was obtained. Therefore, a sputtering system coupled with the selenization process in a vacuum has a strong potential for preparation of high-quality CIGS films. The metallic layers were selenized at various temperatures for 0.5 h. Pure-phased CIGS films were obtained on selenization at 600 ˚C. The crystallinity of the prepared film was further enhanced by increasing the selenization temperature from 400 ˚C to 700 ˚C. With further rising the selenization temperature up to 800 ˚C, the CIGS phase disappeared, Cu_2Se formed and the layer became amorphous like. The lowest surface roughness belongs to the sample selenized at 400 ˚C and the surface roughness of CIGS layers decreased with increasing the selenizing temperature from 500 to 700 ˚C. At 800 ˚C the layer destroyed completely.

REFERENCES

1. C.A. Wolden, J. Kurtin, J.B. Baxter, I. Repins, S.E. Shaheen, J.T. Torvik, A.A. Rockett, V.M. Fthenakis, E.S. Aydil, *Journal of Vacuum Science & Technology A*, **2011**, *29*, 801.
2. S. Niki, M. Contreras, I. Repins, M. Powalla, K. Kushiya, S. Ishizuka, K. Matsubara, *Research and Applications*, **2010**, *18*, 453.
3. M. Klenk, O. Schenker, E. Bucher, *Thin Solid Films*, **2006**, *361-362*, 229.
4. S.R. Kodigala, *Cu (In1-xGax) Se_2 based thin film solar cells*, Academic Press, **2011**.
5. A.M. Gabor, J.R. Tuttle, D.S. Albin, M.A. Contreras, R. Noufi, A.M. Hermann, *Applied Physics Letters*, **1994**, *65*, 198.
6. M. Kemell, M. Ritala, M. Leskelä, *Critical Reviews in Solid State and Materials Sciences*, **2005**, *30*, 1.
7. C. Huang, S.S. Li, W. Shafarman, C.-H. Chang, E. Lambers, L. Rieth, J. Johnson, S. Kim, B. Stanbery, T. Anderson, *Solar energy materials and solar cells*, **2001**, *69*, 131.
8. O. Lundberg, J. Lu, A. Rockett, M. Edoff, L. Stolt, *Journal of Physics and Chemistry of Solids*, **2003**, *64*, 1499.
9. J. Merino, M. León, F. Rueda, R. Diaz, *Thin Solid Films*, **2000**, *361*, 22.

10. C. Xu, H. Zhang, J. Parry, S. Perera, G. Long, H. Zeng, *Solar Energy Materials and Solar Cells*, **2013**, *17*, 357.
11. H.K. Song, S.G. Kim, H.J. Kim, S.K. Kim, K.W. Kang, J.C. Lee, K.H. Yoon, *Solar Energy Materials and Solar Cells*, **2003**, *75*, 145.
12. S.M. Kong, R. Fan, S.H. Jung, C.W. Chung, *Journal of Industrial and Engineering Chemistry*, **2013**, *19*, 1320.
13. S.-C. Chen, D.-H. Hsieh, H. Jiang, Y.-K. Liao, F.-I. Lai, C.-H. Chen, C.W. Luo, J.-Y. Juang, Y.-L. Chueh, K.-H. Wu, *Nanoscale Research Letters*, **2014**, *9*, 280.
14. A. Kampmann, V. Sittinger, J. Rechid, R. Reineke-Koch, *Thin Solid Films*, **2000**, *361–362*, 309.
15. L. Zhang, F.D. Jiang, J.Y. Feng, *Solar Energy Materials and Solar Cells*, **2003**, *80*, 483.
16. M. Ganchev, J. Kois, M. Kaelin, S. Bereznev, E. Tzvetkova, O. Volobujeva, N. Stratieva, A. Tiwari, *Thin Solid Films*, **2006**, *511*, 325.
17. R. Caballero, C. Maffiotte, C. Guillen, *Thin Solid Films*, **2005**, *474*, 70.
18. G. Chen, J. Yang, Y. Chan, L. Yang, W. Huang, *Solar Energy Materials and Solar Cells*, **2009**, *93*, 1351.
19. D. Abou-Ras, G. Kostorz, D. Bremaud, M. Kälin, F. Kurdesau, A. Tiwari, M. Döbeli, *Thin Solid Films*, **2005**, *480*, 433.
20. T. Nakano, T. Suzuki, N. Ohnuki, S. Baba, *Thin Solid Films*, **1998**, *334*, 192.
21. S. Deok Kim, H.J. Kim, K. Hoon Yoon, J. Song, *Solar Energy Materials and Solar Cells*, **2000**, *62*, 357.
22. A. Kinoshita, M. Fukaya, H. Nakanishi, M. Sugiyama, S.F. Chichibu, *Physica Status Solidi (C)*, **2006**, *3*, 2539.